

Without further study, it is difficult to discuss these data quantitatively. However, these results indicated further that for the PSAA system, the metal ions were located closer to each other than for a statistical distribution of metal-metal distances and the metal ions in the CPS and SPS systems have longer metal-metal distances. This shows further that the CPS and SPS do not form ion aggregates or clusters.

**Acknowledgment.** This research was supported by a generous grant from the National Science Foundation (Polymers Program, Grant No. DMR 78-09764). We thank Professor H. Morawetz for many helpful discussions.

## References and Notes

- (1) (a) Abstracted in part from a dissertation to be submitted by Y. Ueba to the Polytechnic Institute of New York in partial fulfillment of the requirements for the degree of Doctor of Philosophy in Polymer Science and Engineering (1980). (b) IREX exchange scholar from the USSR.
- (2) Holliday, L., Ed. "Ionic Polymers"; Applied Science Publishers: London, 1975.
- (3) Eisenberg, A.; King, M. In "Polymer Physics"; Stein, R. S., Ed.; Academic Press: New York, 1977; Vol. 2.
- (4) Eisenberg, A. *Polym. Prepr., Am. Chem. Soc., Div. Polym. Chem.* **1979**, 20 (1), 286.
- (5) Morawetz, H. *Science* **1979**, 202, 405.
- (6) Banks, E.; Okamoto, Y.; Ueba, Y. *J. Appl. Polym. Sci.* **1980**, 25, 359.
- (7) Lundberg, R. D.; Makowski, H. S. *Polym. Prepr., Am. Chem. Soc., Div. Polym. Chem.* **1978**, 19, 287.
- (8) Witt, J. R.; Orsfott, E. I. *J. Inorg. Nucl. Chem.* **1962**, 24, 637.
- (9) Van Uitert, L. G. *J. Electrochem. Soc.* **1960**, 107, 803.
- (10) Eisenberg, A.; Navratil, M. *Macromolecules* **1973**, 6, 604.
- (11) Rigdahl, H.; Eisenberg, A. *Polym. Prepr., Am. Chem. Soc., Div. Polym. Chem.* **1979**, 20 (1), 269.
- (12) Tanner, S. P.; Thomas, D. L. *J. Am. Chem. Soc.* **1974**, 96, 706.
- (13) Reisfeld, R.; Greenberg, E.; Velapoldi, R.; Barnett, B. *J. Chem. Phys.* **1972**, 56, 1698.
- (14) Dawson, R. W.; Kropp, L. J.; Windsor, M. W. *J. Chem. Phys.* **1966**, 45, 2410.
- (15) Nakazawa, E.; Shinoya, S. *J. Chem. Phys.* **1967**, 47, 3211.
- (16) Reisfeld, R.; Boehm, L. *J. Solid State Chem.* **1972**, 4, 417.
- (17) Reisfeld, R.; Greenberg, E.; Biron, E. *J. Solid State Chem.* **1974**, 9, 224.
- (18) Horrocks, W. D., Jr.; Holmquist, B.; Vallee, B. L. *Proc. Natl. Acad. Sci. U.S.A.* **1975**, 72, 4764.
- (19) Förster, T. *Z. Naturforsch., A* **1949**, 4, 321.
- (20) Berlman, I. B. "Energy Transfer Parameters of Aromatic Compounds"; Academic Press: New York, 1973.
- (21) Billmeyer, F. W., Jr. "Textbook of Polymer Science", 2nd ed.; Wiley-Interscience: New York, 1971; p 506.

## Supermolecular Structure and Thermodynamic Properties of Linear and Branched Polyethylenes under Rapid Crystallization Conditions

L. Mandelkern,\* M. Glotin, and R. A. Benson

Department of Chemistry and Institute of Molecular Biophysics, Florida State University, Tallahassee, Florida 32306. Received August 11, 1980

**ABSTRACT:** The crystalline morphology, or supermolecular structure, of polyethylenes crystallized under controlled nonisothermal conditions has been studied by light-scattering techniques. The morphological forms observed can be systematically changed with molecular weight and quenching temperatures and merge in a continuous manner with those previously reported for isothermal crystallization conditions. It is now possible to develop a random lamella-type morphology at much lower molecular weights than heretofore. Moreover, as a consequence of these studies, a variety of superstructures can be developed for the same molecular weight at the same level of crystallinity. Thus the different factors contributing to the properties of semicrystalline polymers can be separated and treated as independent variables. The influence on the morphology of different constitutional factors such as molecular weight, concentration of branch groups, and copolymer concentration is described. The thermodynamic properties of these systems are studied in detail, and it is found that there is no influence of the morphology (as an independent variable) on these properties.

## Introduction

A lamellar crystallite, with its associated amorphous and interfacial regions, represents the elementary structural entity of a homopolymer crystallized from the melt.<sup>1-4</sup> These primary crystallites can, under certain circumstances, be organized into higher levels of crystalline morphology, or supermolecular structure. The commonly observed spherulitic structures are in this category. Detailed studies of linear polyethylene fractions<sup>5-8</sup> have shown that in fact a variety of crystalline morphological forms can be obtained. These develop in a systematic manner as the molecular weight and crystallization temperatures are varied. The main work that has been reported so far<sup>8</sup> covered a molecular weight range from about  $1 \times 10^4$  to  $8 \times 10^6$ , the complete isothermal crystallization range, as well as one rapid (quenched) crystallization procedure. The most perfectly developed spherulites, essentially of the classical type, are observed in the lower molecular weight samples,  $M \lesssim 8.5 \times 10^5$ . In contrast, the higher

molecular weight samples do not display any well-defined morphology under any crystallization conditions. The lower molecular weight, isothermally crystallized samples developed either a poorer spherulitic organization or rod-like forms, depending on the molecular weight and crystallization temperature. The crystalline morphology has been found to be extremely sensitive to molecular weight polydispersity.<sup>7-9</sup>

In contrast to the results for linear polyethylene, an initial study of low-density (branched) polyethylene samples showed that, for unfractionated polymers which were crystallized isothermally at low undercoolings and then cooled to room temperature, spherulitic structures always developed.<sup>10</sup> However, when these samples were quenched from the melt, a variety of morphological forms were observed which depended on the branching concentration and proportion of high molecular weight species present. The most highly branched sampled did not display any well-defined crystalline morphology.<sup>10</sup> However, branched

Table I  
Characterization of Linear Polyethylene Fractions

$M_n \times 10^{-3}$	$M_w \times 10^{-3}$	$M_w \times 10^{-3}$
0.70		
1.14		1.26
1.68		1.93
3.77		4.12
5.6		5.8
	8.6	
11.0		11.5
26.5		27.8
42.0		46.2
72.8		80.8
153		161
179		188.5
217.2		252
445		480
	850	
	1500	
	1890	
	3000	
	6000	
	8000	

and linear fractions gave similar results on quenching since more highly organized structures developed. The isothermal crystallization of the branched samples at the higher temperatures is similar to copolymers, since only relatively small amounts of crystallinity develop over many decades of time. Hence there are complications in interpreting the results because of the large amount of crystallinity that occurs on cooling and the influence of the crystallinity formed at the elevated temperatures on the morphology that subsequently develops.<sup>11</sup> These observations are probably cogent to the anomalies previously discussed, and this aspect of the problem will be treated in a separate report.<sup>11</sup>

Systematic studies of the branched polyethylenes have been hampered in the past because of the lack of detailed quantitative information with respect to molecular constitution and polydispersity. Modern analytical methods such as gel permeation chromatography and <sup>13</sup>C NMR spectroscopy have alleviated these difficulties. All the samples used here have been characterized by these methods. The earlier study of the branched polyethylenes<sup>10</sup> as well as previous work with polymethylene copolymers<sup>12</sup> have pointed out a very strong dependence of the supermolecular structure on the branching concentration and molecular weight distribution.

In the present work we have examined the effect of extending the crystallization range and varying the molecular constitution and polydispersity on the morphological forms and thermodynamic properties. Nonisothermal modes of crystallization were developed. The influence of molecular constitution was assessed by studying linear polyethylene fractions, low-density (branched) polyethylene fractions, and ethylene-butene copolymers. The results for the isothermally crystallized linear polyethylene fractions have already been reported.<sup>8</sup> For the

reasons outlined above, the isothermally crystallized branched polymers require separate treatment; the results of this study will be reported subsequently.<sup>11</sup>

The supermolecular structures have been deduced primarily from the  $H_v$  small-angle light-scattering patterns, SALS,<sup>13,14</sup> complemented when necessary by polarized light microscopy and thin-section transmission electron microscopy.<sup>8,15</sup> As has been recently reported,<sup>4</sup> the polyethylenes display five distinguishable light-scattering patterns which are associated with six different morphological structures. Patterns designated a-c are fourfold symmetric, giving rise to spherulitic structures labeled in the same manner. The spherulitic order deteriorates in the progression a to c. A type-d pattern, which displays some azimuthal dependence of the scattering, is indicative of lamellae organized as thin rods or rodlike aggregates which are also designated as type-d morphological structures. The h-type scattering pattern, which has no angular dependence, does not lead to a unique supermolecular structure. It can be due either to rods whose breadth is comparable to their length, designated as g structures in the ensuing work, or to randomly oriented lamellae which are labeled h. Some form of microscopy must be used to distinguish between these latter two structures. It has been shown that all of the crystalline morphologies that are deduced from the light-scattering patterns are directly confirmed for the same molecular weight and crystallization conditions by transmission electron microscopy using the staining, thin-sectioning technique.<sup>15</sup>

### Experimental Section

The linear polyethylene fractions that were used were either produced in our laboratory or obtained from outside sources. The laboratory methods involved either the liquid-liquid fractionation<sup>16</sup> of Hifax-16 and Hifax-28 (manufactured by the Hercules Powder Co.) for the high molecular weights or column fractionation<sup>16</sup> of Marlex-50 (manufactured by the Phillips Petroleum Co.) for the lower molecular weights. Fractions were also obtained from Societe Nationale des Petroles D'Aquitaine (SNPA) which were prepared and characterized by gel permeation chromatography. The 2000 and 1000 molecular weight samples were obtained from the Petrolite Co. and characterized by gel permeation chromatography. The 700 molecular weight sample was obtained from Polysciences. Viscosity-average molecular weights were determined for certain samples, using the relation given by Chiang.<sup>17</sup> The characteristics of all the fractions used here, many of which were also used in previous work,<sup>8</sup> are given in Table I.

A set of typical low-density (branched) unfractionated commercial samples was also used in this study. Their branching and molecular weight characteristics are given in Table II. Except for samples a and e, all the others were used in studies where the <sup>13</sup>C NMR method established the type and concentration of branches,<sup>18</sup> and the initial morphological results were reported.<sup>10</sup> Only the unique resonances, which can be unequivocally assigned, are used to characterize the sample.<sup>18,19</sup> The molecular weights were determined in the conventional way by gel permeation chromatography.<sup>20</sup>

Also studied were two sets of fractions which were described and prepared by Westerman and Clark.<sup>20,21</sup> These are identified

Table II  
Branching<sup>a</sup> and Molecular Weight Characteristics of Unfractionated Polyethylenes

sample	Et	Bu	Am	total SCB	long-chain branching	total branching	$M_w \times 10^{-5}$	$M_w/M_n$	$(M_w^2/M_n) \times 10^{-5}$
a	1.4	3.6	1.1	6.1	0.9	7.0	1.48	9.6	14.2
b	3.4	4.1	2.2	9.7	2.2	11.9	2.06	5.0	10.0
c	4.4	4.0	2.2	10.6	2.2	12.8	3.46	18.5	64.0
d	0	11.1	1.5	12.6	1.5	14.1	0.94	4.8	4.5
e	3.6	8.3	1.0	12.9	1.6	14.5	9.46	64	605
f	6.0	8.5	1.3	15.8	1.2	17.0	2.6	20	52.0
g	11.3	3.9	0.6	15.8	1.2	17.0	9.5	57	542

<sup>a</sup> Branches per 1000 carbons; based on unique resonance assignments.

Table III  
Branching<sup>a</sup> and Molecular Weight Characteristics of Polyethylene Fractions

sample	Me	Et	Bu	Am	total SCB	long-chain branching	total branching	$M_n \times 10^{-3}$	$M_w \times 10^{-3}$	$M_w/M_n$
A3	1.8	1.1	4.8	0.9	8.6	1.1	9.7		47.6	
A5	1.5	1.5	4.9	0.9	8.8	1.3	10.1		123	
A7	1.3	3.5	5.6	1.0	11.4	1.6	13.0		412	
B4	0	4.9	9.3	0.6	14.8	0.6	15.4	7.13	10.2	1.43
B5	0	3.8	7.9	2.8	14.5	2.4	16.9	9.41	14.5	1.54
B7	0	5.4	8.0	1.2	14.6	0.8	15.4	24.2	113	4.67
B8	0	5.4	9.5	2.2	17.1	2.2	19.3	52.6	866	16.46
B9	0								1610	
B10	0	7.3	7.1	1.2	15.6	1.0	16.6		1730	
P16 <sup>b</sup>	0	21	0	0	21	0	21	14	16	1.14
G25 <sup>b</sup>	0	20	0	0	20	0	20		25	
G75 <sup>b</sup>	0	18	0	0	18	0	18		75	
P108 <sup>b</sup>	0	22	0	0	22	0	22	82	108	1.5
P194 <sup>b</sup>	0	20	0	0	20	0	20	126	194	1.53
P420A <sup>b</sup>	0	22	0	0	22	0	22	226	413	1.84

<sup>a</sup> Branching per 1000 carbons; based on unique resonance assignments. <sup>b</sup> Hydrogenated polybutadiene.

Table IV  
Characterization of Compositionally Fractionated Ethylene-Butene Copolymers

mol % Et	$M_n$	mol % Et	$M_n$
0.33	32 000	2.00	40 000
0.61	50 000	2.72	70 000
1.00	32 000	2.94	26 000

as the A and B series,<sup>21</sup> and their branching and molecular weight characteristics are given in Table III. Unfractionated sample e is the parent of the B series. It should be noted that the A series contains methyl side groups, while the B series does not. For either set, the total branching concentration is not very dependent on the molecular weight.

A series of hydrogenated polybutadiene samples was also studied, and their characteristics are listed in Table III. Those with the prefix P were obtained from the Phillips Petroleum Co. Two samples, G25 and G75, were kindly donated to us by Professor William Graessley of Northwestern University. Sample P420A represents a refractionation, by liquid-liquid methods, of the original material. These polymers have a narrow molecular weight distribution as a consequence of being anionically polymerized. Since 1,2 butadiene additions can take place, random, isolated ethyl groups are formed after hydrogenation. <sup>13</sup>C NMR analysis indicates that about 2.0 mol % ethyl side groups are present independent of molecular weight. For crystallization purposes, this class of polymers is thus properly thought of as random ethylene-1-butene copolymers. They should not be misconstrued to be, or treated as, homopolymers.<sup>22</sup>

In addition to the above, some molecular weight fractions of compositionally fractionated ethylene-butene copolymers were also studied. Their pertinent characteristics are listed in Table IV. They were prepared from commercially available copolymers by liquid-liquid fractionation followed by crystallization from dilute solution to attain compositional fractionation.<sup>23</sup> These samples represent a set of compositionally fractionated copolymers with a restricted molecular weight range. It is the first time that the crystallization of such systems has been studied so that compositional fractionation is avoided during crystallization.

The SALS patterns were obtained by using a photometer similar to the one described by Stein.<sup>13,14</sup> The theoretical basis for the deduction of the supermolecular structure from the light-scattering patterns has been previously summarized.<sup>8</sup> It is based on established theory.<sup>13,24,25</sup> Following the previous discussion, the letter designation that we shall be using henceforth will refer to the morphological form.

The densities of the samples were obtained by using a 2-propanol/water gradient column at 23 °C. These values were converted to degree of crystallinity by the specific-volume relation given by Chiang and Flory.<sup>26</sup> The enthalpies of fusion and melting

temperatures were obtained with a differential scanning calorimeter (Perkin-Elmer DSC-2B), using procedures previously described.<sup>27,28</sup> In calculating the degree of crystallinity from these data, the enthalpy of fusion of the perfect crystal was taken as 69 cal gm<sup>-1</sup>. For the broadly melting branched polymers it is necessary to scan as wide a temperature range as possible. Hence the low-temperature accessory was used, with liquid nitrogen as refrigerant.

The light-scattering samples were in the form of thin films. These were prepared by placing the polymer between two 20-μm-thick aluminum foils and pressing at ca. 160 °C between the plates of a Carver press. The pressure applied was between 5000 and 15 000 lb in.<sup>-2</sup>, depending on molecular weight. This pressure produced films between 25 and 40 μm thick. The film thus formed was first cooled rapidly to room temperature. Then, while still between the aluminum foil, it was returned to the hot platen of the press for ease in accessibility for the subsequent quenching. After a short time period, allowing for the sample to become completely molten, it was quickly plunged into a refrigerant set at a predetermined temperature. A wide range of quenching temperatures was used in this work. The lowest temperature, resulting in the most rapid cooling rate, was achieved by quenching into *n*-pentane at its melting temperature. Temperatures between -70 and 0 °C were obtained with 2-propanol, cooled with solid CO<sub>2</sub>. Water baths were used for temperatures between 0 and 100 °C. Some samples were prepared by quenching between 100 and 105 °C in a thermostated ethylene glycol bath for a sufficiently long time to ensure complete crystallization. The necessary times were determined by independent crystallization kinetics. These ranged from a few minutes to several hours, depending on the sample. Further crystallization ensued on subsequent cooling of these samples to room temperature.

We have arbitrarily defined isothermal crystallization temperatures as corresponding to conditions where at least 10 min elapse before crystallization is detected. This temperature region is not studied in the present work for any of the sample classifications. Attention is focused on the nonisothermal temperature region for the purpose of obtaining major changes in morphological form with the same sample. The temperature of the refrigerant does not correspond to the crystallization temperature, since crystallization undoubtedly ensues before this temperature is reached. If any differences in morphology are observed, they should properly be attributed to differences in cooling rate. This type of crystallization experiment is clearly a subjective one. Its worthiness can only be judged by the reproducibility of the results and their significance.

## Results and Discussion

**Crystalline Morphology. Linear Polyethylene Fractions.** In the previous work the nonisothermal crystallization of linear polyethylene was limited to one

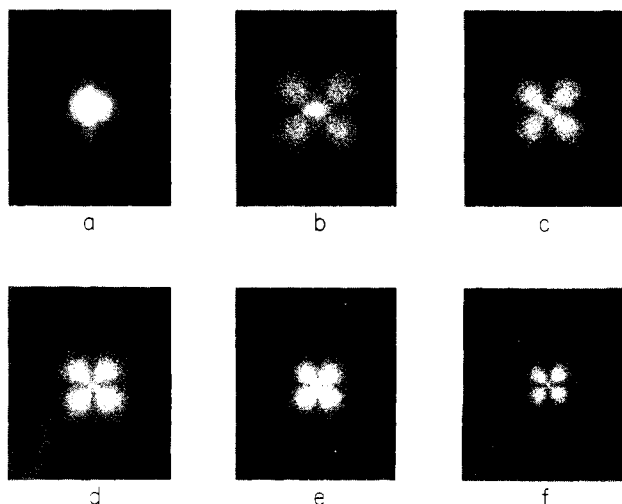


**Figure 1.**  $H_v$  small-angle light-scattering patterns for the  $M = 1.61 \times 10^5$  molecular weight fraction of linear polyethylene crystallized nonisothermally at the following quenching temperatures ( $^{\circ}\text{C}$ ): (a)  $-130$ ; (b)  $-70$ ; (c)  $-40$ ; (d)  $+40$ ; (e)  $+80$ ; (f)  $+110$ .

procedure, namely, transferring into an isopropyl alcohol/dry ice mixture.<sup>8</sup> It was found that for molecular weight fractions less than  $8.5 \times 10^5$ , well-defined type-a spherulitic structures are observed. For  $M = 8.5 \times 10^5$  and slightly higher, although spherulites are still observed, the order has deteriorated into a type-b spherulite. For  $M$  greater than  $2 \times 10^6$ , an h-type morphology corresponding to randomly oriented lamellae is deduced from the light-scattering pattern. Molecular weights between  $1 \times 10^6$  and  $2 \times 10^6$  represented a transition region, with poorly developed spherulites, random structures, or rodlike structures being reported.<sup>5,28</sup> In this range, the morphology is apparently very sensitive to molecular weight or molecular weight distribution as well as to the details of film thickness and quenching procedure. The reason for the transition region in this particular molecular weight range will become clearer when we examine the new results that are reported below.

In the present work, we have found that by varying the cooling rate, or quenching conditions, it was possible to develop major morphological changes. These kinds of experiments represent the core of the results that we report here. A typical set of light-scattering patterns that can be obtained is shown in Figure 1 for a linear polyethylene fraction,  $M = 1.61 \times 10^5$ . The lowest quenching temperature,  $-130^{\circ}\text{C}$ , results in a sample which displays a circularly symmetric light-scattering pattern (Figure 1a), which is shown to correspond to the h-type random lamellae morphology. Increasing the quenching temperature produces samples whose spherulitic morphology becomes progressively better defined. For example, when quenched at  $-70^{\circ}\text{C}$  type-c spherulite is observed (Figure 1b). A type-b spherulite is observed at  $-40^{\circ}\text{C}$  (Figure 1c). For quenching temperatures above  $20^{\circ}\text{C}$ , type-a spherulites are observed (Figure 1d–f). Accompanying this increase in spherulitic order is a continuous increase in their radii, as determined by the angular position of the intensity maximum.<sup>13</sup> For example, for quenching temperatures from  $-70$  to  $+110^{\circ}\text{C}$  (the spherulite-forming range for this fraction), the spherulite radii increase from  $2.5$  to  $12\ \mu\text{m}$ .

The results for the complete molecular weight range studied,  $1.0 \times 10^3$  to  $8 \times 10^6$ , can be plotted as a morphological map, as is shown in Figure 2. In this study we encompass an approximately 8000-fold range in molecular weight. The temperature axis in this plot is composed of

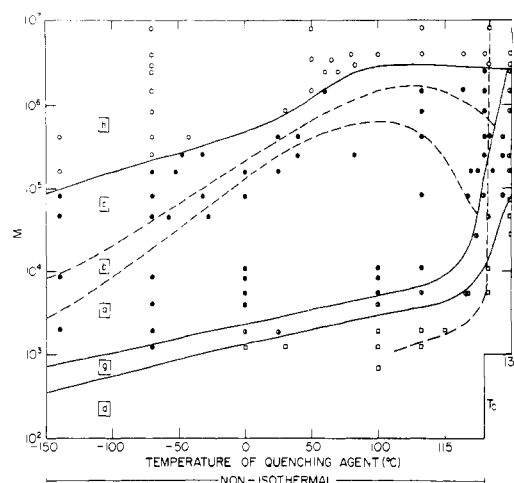


**Figure 2.** Morphological map for molecular weight fractions of linear polyethylene. Plot of molecular weight against either quenching or isothermal crystallization temperatures. Morphological forms indicated by letters as defined in text.

both the quenching temperatures, representing nonisothermal crystallization, and the isothermal crystallization range. The data for the isothermal crystallization are primarily from previous work,<sup>8</sup> with a few additional data points which continue the trends already established. The isothermal range represents but a small portion of the total temperature range, reflecting the well-known limitation of isothermal crystallization for linear polyethylene.<sup>29</sup> The curve drawn between the g and b regions, in the isothermal range, represents what has been termed regimes I and II, respectively. The morphological map of Figure 2 demonstrates the wide range in morphologies that can be developed for a given molecular weight. Except for the very highest molecular weights, where the h-type morphology is observed under all crystallization conditions, the cooling rate exerts an important influence on the morphology. However, the nonisothermal results merge smoothly into the isothermal crystallization range. One can now obtain samples with no organized supermolecular structure for all fractions of  $M = 1.61 \times 10^5$  or greater. As the molecular weight is increased, the range of quenching temperatures within which spherulites are observed is continuously reduced. For molecular weights greater than about  $2 \times 10^6$ , no spherulitic morphology is developed, as was previously reported.<sup>8</sup> Several general trends are displayed. At a fixed quenching temperature, the morphological order decreases with increasing molecular weight in a fairly dramatic way. Except for the highest molecular weights, where no changes are observed, the morphological order, including spherulite structure, increases as the quenching temperature is raised. By examining Figure 2 we find that the previously reported quenching experiments correspond to  $60$ – $70^{\circ}\text{C}$  on the present scale. With this identification, the morphology/molecular weight observations bear a one-to-one relation between the two works. The reason for the transition region, previously described in the vicinity of  $(1\text{--}2) \times 10^6$ , now becomes clear. At this quenching temperature there is an ill-defined boundary between c-type spherulites and random lamellae—hence the irreproducibility between different investigators. Despite the subjectivity of the nonisothermal quenching type of crystallization, a major goal has been accomplished in that a more diverse set of supermolecular structures can be developed for the same molecular weight in relation to what can be accomplished by isothermal crystallization.

**Branched Polyethylene Fractions.** Previous results have shown that for the branched polyethylenes, molecular

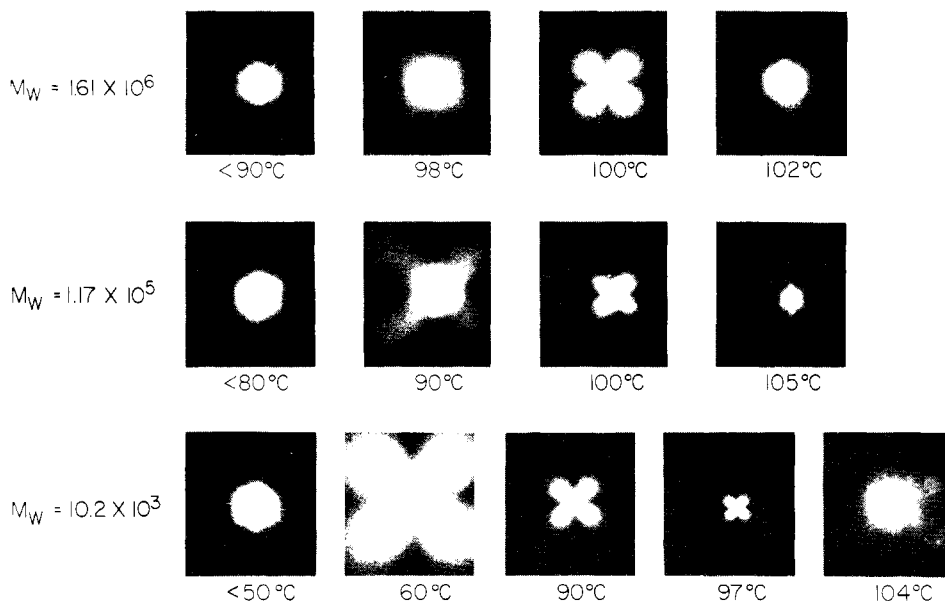


**Figure 3.**  $H_v$  small-angle light-scattering patterns for several molecular weight fractions of B series of low-density (branched) polyethylenes crystallized nonisothermally at indicated quenching temperatures.

weight, polydispersity, and branching are the major molecular factors which influence morphology.<sup>10</sup> To sort out these different factors we have focused initial attention on the study of a series of molecular weight fractions, each group of which has essentially the same branching concentration and whose properties are given in Tables III and IV.

A typical set of SALS patterns for the B series of fractions is shown in Figure 3. Here the branching concentration is about 1.5 mol % for all molecular weights. Even a cursory examination of the patterns shows that a wide variety of morphological forms are developed. In addition, for this set of fractions there is a systematic dependence of the morphology on molecular weight. Quenching at low temperatures always produces an h-type SALS pattern. The limiting temperature below which this pattern is observed increases with increasing molecular weight. At a sufficiently high molecular weight,  $M_w = 2 \times 10^6$  in this case, this type of pattern is observed for all nonisothermal crystallization conditions. For the lower molecular weights, as the quenching temperature is increased above the limiting values, spherulitic-type SALS patterns develop, with progressively increasing order, as the temperature is increased. However, when the quenching temperature is increased above about 100 °C, depending on molecular weight, the spherulitic type of SALS pattern is lost. The patterns have again become circularly symmetric under these conditions. Polarized light microscopy reveals that under these conditions the lowest molecular weight sample, B4 ( $M_w = 10.2 \times 10^3$ ), has developed structures with some degree of preferred orientation; precise observations are limited by the weakness of the birefringence. The light-scattering pattern from this low molecular weight sample is thus best interpreted as corresponding to a d-type morphology. However, all of the higher molecular weight samples, when examined by polarized light microscopy after being crystallized under similar conditions, show little evidence of birefringence and no organized structures. These morphologies appear to be of the h type on this basis. However, as described below, confirmation by electron microscopy is needed for a more definite conclusion.

The morphological map that results from the light-scattering patterns for this series of fractions is given in

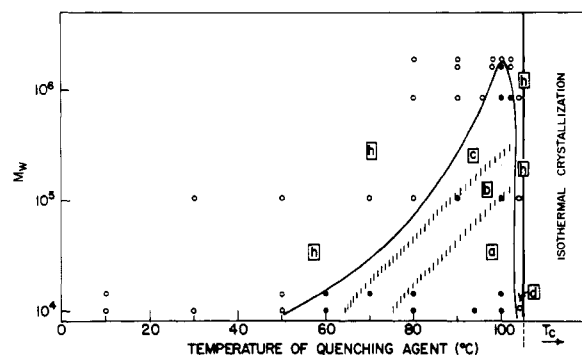


**Figure 4.** Morphological map for molecular weight fractions of low-density (branched) B series polyethylene crystallized nonisothermally. Plot of molecular weight against quenching temperature. Solid line delineates region of spherulite formation. Morphological forms indicated by letters as defined in text.

Figure 4. The isothermal crystallization region is independently defined by kinetic experiments.<sup>11</sup> We limit our attention to the results obtained at lower, nonisothermal crystallization temperatures. There is a typical dome-shaped region in this plot within which spherulites are observed; i.e., there is a restricted domain of molecular weights and quenching temperatures which yield spherulitic structures. The lower the molecular weight, the larger the temperature range within which spherulites form. This range narrows with increasing molecular weight, so that eventually a molecular weight is reached above which spherulites are not formed. The high-temperature boundary remains approximately constant; it is the low-temperature boundary which decreases with increasing chain length. Within the spherulite-forming domain, better defined or more ordered structures, i.e., a types, are favored by lower molecular weight and higher quenching temperatures.

When samples are crystallized outside the dome, at either higher or lower temperatures, a circularly symmetric h-type SALS pattern is observed. This type pattern does not lead to a unique morphological form and other methods need to be used. Polarized light microscopy was not definitive, and thin-section transmission electron microscopy was used.<sup>15</sup> Two samples of the B7 fraction,  $M_w = 1.13 \times 10^5$ , one quenched into a 2-propanol/dry ice mixture

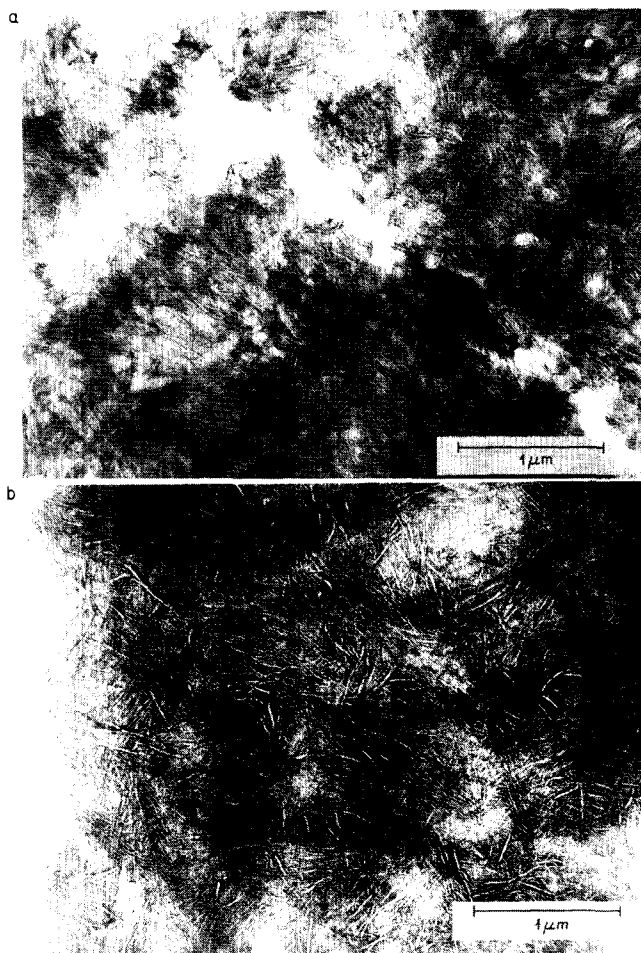


**Figure 5.** Thin-section transmission of electron micrographs of low-density (branched) polyethylene fraction B7: (a) quenched at 0 °C; (b) quenched at 105 °C.

and the other crystallized at 105 °C and cooled to room temperature, were studied. These two conditions represent, respectively, the low- and high-temperature sides of the dome. The corresponding electron micrographs are given in Figure 5.<sup>39</sup> The existence of lamellae is clearly indicated in both samples. They are not, however, organized into any well-defined structures and hence correspond to an h-type morphology, i.e., random lamellae. These drastically different modes of crystallization yield the same h-type SALS patterns and general morphology. The lamellae formed at the low temperatures are much more twisted, or curved, than those formed at the high temperatures, which are relatively straight. These characteristics are indicative of differences in the lamellar growth mechanisms in the two cases while the same gross morphology or disorganized structure results.<sup>40</sup>

If we compare these results with those for linear polyethylene fractions, we find that, although the spherulitic morphology is lost after high-temperature crystallization for both types, it only occurs in the isothermal range for the linear polymer. Here, except for the very high molecular weights, well-defined morphological forms, the d- and g-type rods, are observed.<sup>8</sup> At the low temperatures for the branched fractions, the spherulitic morphology is lost to the random structures for the lowest molecular weight studied for this branching concentration,  $M_w = 1.0 \times 10^4$ . For the linear fractions this change cannot be accomplished until  $M = 1.6 \times 10^5$ . If the linear fractions are taken as a reference, then from the point of view of the

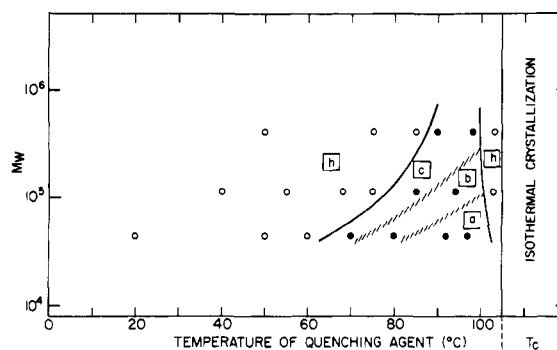


**Figure 6.** Morphological map for molecular weight fractions of low-density (branched) A series polyethylene crystallized non-isothermally. Plot of molecular weight against quenching temperature. Solid line delineates region of spherulite formation. Morphological forms indicated by letters as defined in text.

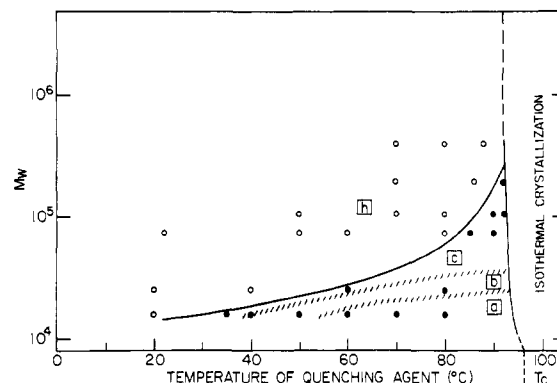


**Figure 7.** Morphological map for narrow molecular weight, hydrogenated polybutadiene samples crystallized nonisothermally. Plot of molecular weight against quenching temperature. Solid line delineates region of spherulite formation. Morphological forms indicated by letters as defined in text.

morphology produced, the branched samples can be considered to behave as though they were of higher molecular weight.

The morphological map for the A series of branched polyethylene fractions is given in Figure 6. These fractions contain about 1 mol % branches. The general features of this map are similar to those of the B series. However, the molecular weights in the A series are not sufficiently high to allow for a specification of the limiting molecular weight for spherulite formation. However, the trend in the data is such that a cutoff and a dome-shaped region are expected, as in the B series. The morphological results for the hydrogenated polybutadiene series are given in Figure 7. Here each fraction has a very narrow molecular weight distribution and contains about 2.0 mol % ethyl side groups. The limiting molecular weight for spherulite formation has been reduced from  $2 \times 10^6$  for the B series to about  $2 \times 10^5$  with this increased branching concentration. Thus, what would appear to be a very small change in branching concentration has a major effect on morphology in the higher molecular weights. The lowest molecular weights remain essentially unaffected. For the hydrogenated polybutadienes the spherulitic morphology does not disappear on the high-temperature side of the diagram in the nonisothermal region, as was found for the A and B series. This behavior is similar to that of the linear fractions for which loss of spherulitic morphology at high temperature occurs in the isothermal crystallization range. This similarity may be related to the relatively narrow molecular weight distributions as compared with the dispersity of the branched polyethylene fractions.<sup>21</sup>

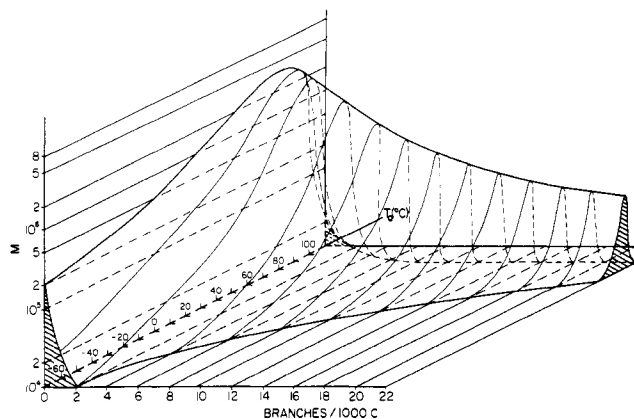


**Figure 8.** Three-dimensional, schematic morphological map for nonisothermal crystallization of polyethylene. Axes are molecular weight, branching concentration, and quenching temperature. The curved, dome-shaped regions define the volume within which spherulitic structures are formed; outside this volume there is no defined morphology.

The morphological results that have been presented for the three sets of fractions have indicated some general trends with regard to molecular weight and branching concentration. The influence of branching concentration was further confirmed by quenching experiments with the ethylene-1-butene compositionally fractionated copolymers. The results described above allow one to construct a schematic three-dimensional morphological map, as is illustrated in Figure 8. In this highly schematic diagram, the variables are the molecular weight, branching concentration, and quenching temperature. The surface that is drawn represents the boundary between spherulite formation and random lamellae. Within the surface, spherulites are formed; beyond the boundary the random structure is observed. Each section at constant branching concentration represents the dome-shaped regions that have been discussed previously. The surface drawn is clearly schematic in character, not to be taken in detail, but is consistent with major results that have been reported. It summarizes the facts that, as the branching concentration is increased, the molecular weight within which spherulites can be formed markedly decreases. If the trend continues, then a branching concentration and/or molecular weight will be reached which does not allow spherulite formation at all. The earlier reports of Jackson and Flory<sup>12</sup> of spherulite formation in high molecular weight diazoalkane copolymers are consistent with these conclusions. At the lower molecular weights, the range of quenching temperatures within which spherulites are formed decreases with molecular weight.

**Unfractionated Branched Polyethylenes.** We have previously reported, based on only one quenching procedure, that for unfractionated branched polyethylenes the molecular weight polydispersity was a major factor in influencing the supermolecular structure. Of particular interest was the influence of the relative proportion of the high molecular weight species. To further augment this work, changes in the crystalline morphology with the quenching temperature were studied for the set of low-density (branched) polyethylenes listed in Table II. The results for this extended range of crystallization conditions are presented in Figure 9. The isothermal crystallization range of this set of samples is delineated by the upper temperature limit of crystallization in the present study. From the map in Figure 9, two very important conclusions can immediately be made. As was found for fractions, increasing the branching concentration reduces the tem-

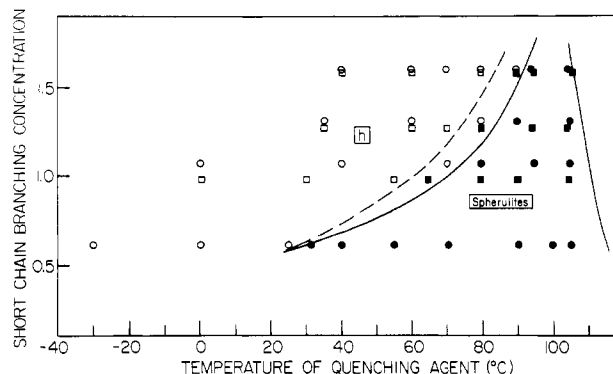


**Figure 9.** Morphological map for unfractionated, low-density (branched) polyethylenes crystallized nonisothermally. Plot of short-chain branching concentration against quenching temperature. Samples characterized in Table II. (●, ■) spherulites; (○, □) random lamellae. Solid and dashed curves delineate morphological transition for high and low values of  $M_w^2/M_n$ , respectively.

perature range over which spherulites can be formed. However, in contrast to the behavior of fractions, there is no loss of spherulitic morphology at the high quenching temperatures. This result is best discussed in connection with the study of isothermal crystallization and the influence of crystallization upon cooling on the morphological form.<sup>11</sup>

The seven unfractionated samples were selected for study so that there were three pairs, each of which has very similar branching concentrations. Samples f and g contain about 1.7 mol % branches; d and e contain about 1.4 mol %; b and c contain about 1.2 mol %. The samples group in the same way if only the short-chain branching is considered. Sample a was selected for its relatively low branching concentration, 0.7 mol %. Despite the close similarity in branching concentration for a given pair, the quenching temperature interval over which the crystalline morphology changes from a spherulitic type to random lamellae is different. For example, for sample d these morphological changes occur between 70 and 80 °C, while for sample e, which has the same branching concentration, this transitional range is about 10 °C higher. Qualitatively similar results are found for samples b and c. Here the transitional ranges are 55–65 and 70–80 °C, respectively. For the pairs f and g these temperature ranges are 80–90 and 90–95 °C. The transition occurs at a much lower temperature for sample a because of its greatly reduced branching concentration.

To understand the difference for the paired samples with the same branching content, we recall the extreme sensitivity of morphology to molecular weight polydispersity observed for linear polyethylenes.<sup>7-9</sup> In a mixture of a spherulite-forming fraction with a non-spherulite-forming high molecular weight fraction, the addition of only small amounts of the latter species was sufficient to disrupt and destroy the well-developed spherulitic structure.<sup>7</sup> In the low molecular weight region, the deliberate broadening of the distribution with species whose molecular weight was either slightly less or slightly greater than the non-spherulitic-forming fraction induced spherulite formation under the same crystallization conditions.<sup>9</sup> In the earlier study of branched polyethylenes,<sup>10</sup> samples having a distribution containing significantly high molecular weight portions gave more disordered structures when rapidly crystallized. It was found convenient, without any theoretical basis, to introduce the variable  $M_w^2/M_n$  to express the influence of the high molecular weight species on the resulting morphology. When the

samples studied here are examined from this point of view, then as the molecular weight data in Table I indicate, the pairs b,c, d,e, and f,g each have the same branching content but widely different values of  $M_w/M_n$ . The sample in each group which has the larger value of this quantity has a higher morphological transition temperature. The solid and dashed curves delineate the morphological transition temperatures for the high and low values of the quantity  $M_w/M_n$ . The previous results<sup>10</sup> are compatible with the data of Figure 9 if the quenching temperature is taken to be 70 °C. Thus the lower the  $M_w$  for the same branching concentration, the greater the range of quenching temperatures wherein spherulites can be developed. Or, at a fixed quenching temperature, spherulites can be developed at a higher branching concentration the lower the molecular weight. For the sake of clarity, we have omitted from Figure 9 the changes in the internal spherulite ordering that are observed. However, the general trends that were observed with the molecular weight fractions are followed. The spherulite order or perfection decreases as the branching concentration is increased or the quenching temperature is lowered.

**Morphology Summary.** The detailed study of the influence of molecular weight, polydispersity, and branching concentration that has been described above allows for some general conclusions to be made with respect to the conditions for the different morphological structures to develop. For linear polyethylene, spherulitic structures are only produced for limited molecular weights under restricted crystallization conditions.<sup>6,8</sup> For crystallization conducted under rapid cooling conditions, as has been emphasized here, further restrictions are imposed on spherulite formation. These are further enhanced by increasing the molecular weight, for fractions, increasing the branching concentration, or increasing the proportion of the high molecular weight species. In those situations where spherulites are actually produced, their internal order and size can be directly related to the quenching temperature and molecular constitutions. Increasing the quenching temperature results in the more highly ordered and larger spherulites. For a given quenching temperature, increasing the molecular weight or the branching concentration results in a decrease in spherulitic order and size.

For both the linear and branched molecular weight fractions, the spherulitic morphology can be lost either at low quenching temperatures or at high crystallization temperatures.<sup>8,10</sup> The morphologies that are observed are either rodlike structures or random lamellae, depending on the molecular weight and structure. For the unfractionated, branched polyethylenes the spherulitic morphology is lost only when the samples are quenched from the melt into low-temperature refrigerant.

For all the structural types, as the quenching temperature is decreased so that the conditions for the transition from spherulites to random lamellae are approached, the size of the spherulites becomes very small. Under these conditions it is theoretically possible that the h-type light-scattering patterns correspond to spherulites of extremely small size. However, the thin-section transmission electron microscopy for the linear polyethylene<sup>15</sup> as well as the branched polyethylene demonstrates that spherulites are not formed under these crystallization conditions. Well-defined lamellae of limited lateral extent whose orientations are uncorrelated are observed. Although the main crystallization mode that has been employed here is not amenable to simple analysis, it has allowed different morphological forms to be developed for the same sample under controlled and reproducible conditions.

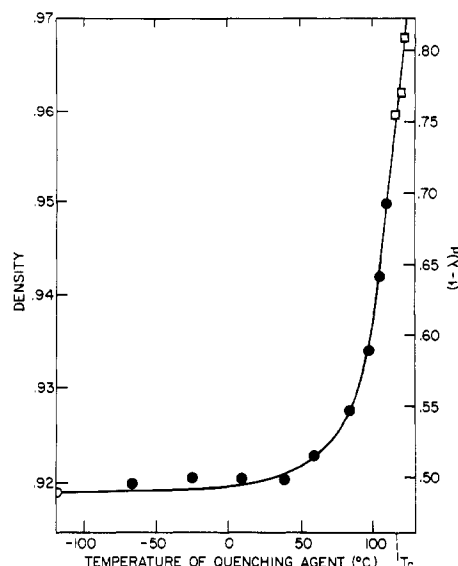


**Figure 10.** Plot of density and degree of crystallinity for an  $M_w = 1.61 \times 10^5$  linear polyethylene molecular weight fraction as a function of either quenching or isothermal crystallization temperature: (○) h-type morphology; (●) spherulites; (□) g-type morphology.

**Properties. Density.** Since a spectrum of morphological forms can be reproducibly developed in a given sample by varying crystallization conditions, we are in a position to assess the influence of the supermolecular structure on properties. We focus attention on thermodynamic properties such as the melting point, enthalpy of fusion, and density.

In the discussion of the density, we take as a convenient reference point the results for the linear molecular weight fraction  $M_w = 1.61 \times 10^5$ . This fraction represents the lowest molecular weight of linear polyethylene in which random lamellae have been developed to date by rapid crystallization. The degree of crystallinity and the density of this fraction are plotted in Figure 10 as a function of the quenching temperature. In addition, three points obtained for this sample subsequent to isothermal crystallization at the indicated temperatures are also given.<sup>8</sup> The morphological map of Figure 2 indicates that for this fraction, random lamellae and all spherulite types are developed on quenching at appropriate temperatures; after isothermal crystallization a g-type, rodlike morphology is observed. It is clear from Figure 10 that the density is continuous over this whole crystallization range and over the different morphological forms. The morphology does not appear to directly influence the density, which is primarily determined by the crystallization conditions. Quenching at temperatures below ca. 30 °C produces samples which have a constant level of crystallinity, about 0.50 at room temperature, but morphologies which differ as widely as randomly arranged lamellae to the best organized a-type spherulites. It has thus been possible to separate the level of crystallinity and supermolecular structure for the same sample and to treat each as an independent variable.

Similar experimental results have been reported for other molecular weight fractions of the linear polymer.<sup>4</sup> For  $M_w = 2.78 \times 10^4$ , the density curve is also continuous; but only spherulitic structures are observed on quenching this lower molecular weight fraction. The level of crystallinity is 0.62 after quenching at temperatures below about 30 °C, which is greater than that for the higher molecular weight fraction. Under these crystallization conditions, the three different spherulitic morphologies are

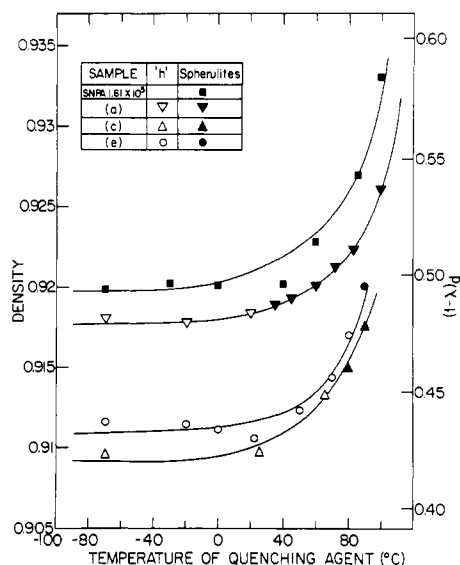


**Figure 11.** Plot of density and degree of crystallinity for linear polyethylene fraction and three unfractionated low-density (branched) samples. Sample designation from Table II and morphologies indicated in figure.

observed, but the density remains constant. A higher molecular weight fraction,  $M_w = 1.50 \times 10^6$ , yields a density curve similar to that in Figure 10 for the lower crystallization temperatures and yields only slightly higher densities in the isothermal range. For this fraction, samples which lack an organized crystalline morphology have the same density as those in which spherulites are developed. This phenomenon appears to be fairly general for linear polyethylene.

Typical results for the unfractionated branched polyethylenes are given in Figure 11. Here the densities, or degree of crystallinity, are plotted as a function of the quenching temperature. For comparative purposes, the results for the linear fraction  $M_w = 1.61 \times 10^5$  are also shown. The density for each sample is continuous with the quenching temperature and does not reflect the morphological changes that occur. A general trend is evidenced in that an increase in the level of branching reduces the level of crystallinity, as would be expected from copolymer theory.<sup>30,31</sup> The lowest degree of crystallinity in Figure 11 is about 0.41–0.42 for the B series (~1.5 mol % branch groups). The degree of crystallinity is reduced to 0.36 for the narrow molecular weight distribution, hydrogenated polybutadienes (not shown), which contain about 2.0 mol %, randomly distributed ethyl branches. When the density is examined against the branching concentration, at any temperature, it is evident that a limiting value has not as yet been achieved at the level of 2 mol % co-unit content.

The influence of molecular weight on the density of a set of fractions of approximately constant branching content is illustrated in the upper portion of Figure 12 for the B series. We note that over the extremes in crystallization conditions and the wide range in molecular weights, the densities do not vary by more than 0.01 units. This value corresponds only to about a 10% change in the total range in the degree of crystallinity. For fractions of this branching concentration, although the molecular weight range is similar to that studied for the linear polymer, no sensible effect of either molecular weight or morphological form<sup>32</sup> is found for the same crystallization conditions. The hydrogenated polybutadienes show the same invariance of density to molecular weight for the same crystallization conditions, except for the very lowest molecular weight,

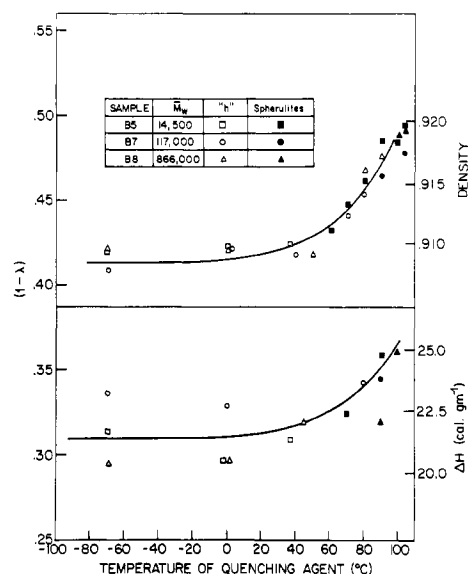


**Figure 12.** Plot of densities, enthalpies of fusion, and degree of crystallinity against quenching temperatures for several fractions of B series. Molecular weights and morphologies indicated in figure.

where a small effect is noted. The density thus appears to be determined primarily by the concentration of branch groups. For the linear polymers, the degree of crystallinity changes by about 30% for the most rapid crystallization. In accord with the previous results for the branched and linear polymers, this series of fractions vividly illustrates that the morphology does not influence the density.

**Enthalpies of Fusion.** The melting of branched polyethylenes and of random ethylene copolymers is characterized by broad fusion curves because of their copolymeric character.<sup>33</sup> The fusion process can easily encompass a range of the order of 100 °C. A recent Raman spectroscopic study has shown that the onset of melting for the branched polyethylenes studied can be detected as low as -20 °C.<sup>34</sup> Thus the melting endotherms will be expected to be very broad, a factor which will introduce an element of difficulty in integrating the differential calorimetry scan to obtain the heat of fusion. In this situation a DSC scan starting at room temperature will not yield an accurate measure of the enthalpy of fusion since a portion of the melting endotherm would not be taken into account and the base line chosen will be inaccurate.<sup>41</sup> Similar observations have been reported for rapidly crystallized high molecular weight linear polyethylene fractions.<sup>35</sup> This problem was alleviated in the present work by starting the DSC scan at a temperature in the vicinity of 180 to 200 K and establishing a base line by obtaining the melting endotherm for both the sample of interest and a reference linear polyethylene treated in the same manner.

A typical set of results, in the form of a DSC trace for the unfractionated branched sample, g, is given in Figure 13. This sample was initially quenched at -130 °C. The onset of melting can be easily detected by the departure from the base line, and the necessary integration carried out. The small maximum in the vicinity of 330 K represents the melting of those crystallites which formed after quenching, i.e., while the sample was brought up to or stored at room temperature. A similar thermal behavior has been reported for linear polyethylene.<sup>36</sup> The amount of crystallinity developed in the branched samples subsequent to quenching and storage is on the order of 1%. This very small but detectable contribution to the total

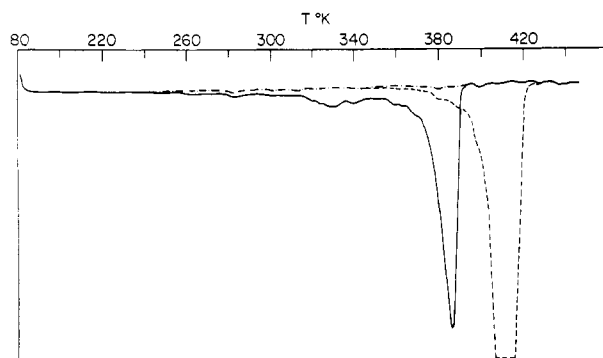


**Figure 13.** DSC scan for low-density (branched) polyethylene (sample g) after quenching at  $-130^{\circ}\text{C}$  (—); unfractionated linear polyethylene (---); base line chosen (---).

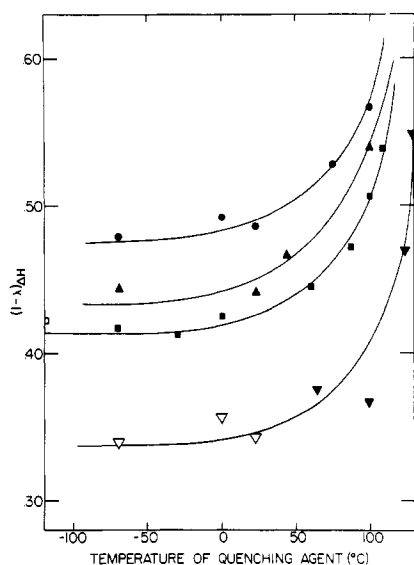


**Figure 14.** Degree of crystallinity, as determined from enthalpy of fusion measurements, as a function of quenching temperature for linear polyethylene fractions.  $M_w = 2.78 \times 10^4$ : (●) spherulites;  $M_w = 4.62 \times 10^4$ : (▲) spherulites;  $M_w = 1.61 \times 10^5$ : (■) spherulites, (□) h-type morphology;  $M_w = 1.89 \times 10^6$ : (▼) spherulites, (▽) h-type morphology.

crystallinity will not sensibly affect the morphology or properties which are studied here at room temperature.

The degree of crystallinity, calculated from the enthalpy of fusion, for a range of linear polyethylene molecular weight fractions is plotted against the quenching temperature in Figure 14. Following the density results, continuous curves are obtained despite the fact that there are significant changes in the crystalline morphology in the higher molecular weight samples. It is again confirmed that increasing the molecular weight reduces the level of crystallinity, which increases at the higher quenching temperature. Thus the degree of crystallinity calculated from either density or enthalpy of fusion measurements depends in a similar manner on molecular weight, quenching temperature, and morphology—although, as we shall discuss below, the two methods do not always give concordant quantitative results.

The enthalpy of fusion measurements for the low-density (branched) polyethylenes bear the same relationship to the density measurements as in the case of the linear polymers. For the unfractionated samples (not shown here) the enthalpies of fusion follow the same functional form as the density plots of Figure 11. They are insensitive to morphology and only depend on the branching concentration and quenching temperature. The results for

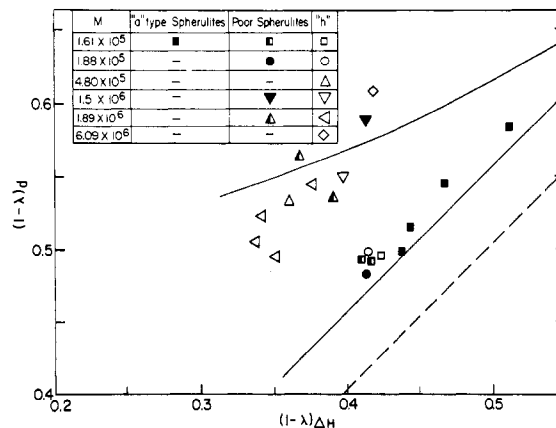


**Figure 15.** Plot of degree of crystallinity from density  $(1 - \lambda)_d$  against degree of crystallinity from enthalpy of fusion  $(1 - \lambda)_{\Delta H}$  for linear polyethylene fractions. Symbols for molecular weights and morphologies indicated in figure.

the B series of molecular weight fractions are given in the lower part of Figure 12. At this branching concentration the enthalpies of fusion do not depend on either molecular weight or crystalline morphology, in accord with the density results. The similarity of the two plots in Figure 12 is quite apparent.

The conclusion made here that the degree of crystallinity calculated from either the enthalpy of fusion or the density does not depend on the morphology is in agreement with previous reports for similarly constituted samples crystallized in a different manner.<sup>4,8,10</sup> However, the two methods are not always in accord; it was previously argued that whether or not agreement was observed depended solely on the morphology.<sup>8</sup> From the restricted data available for linear polyethylene fractions, it was concluded that the two quantities were in essential agreement for well-organized morphologies but that  $(1 - \lambda)_d$  was greater than  $(1 - \lambda)_{\Delta H}$  for samples with disordered supermolecular structures, such as random lamellae or poorly organized spherulites. The restriction on the data resulted because the main morphological changes were accomplished by varying the molecular weight in the earlier work. The disordered structures were favored by the higher molecular weights. The rapid-crystallization methods employed here not only allowed the disordered morphologies to be obtained with much lower molecular weights, but the same fraction could be crystallized in different ways so as to yield virtually all possible superstructures.

The degrees of crystallinity calculated from both methods can now be included with the previous compilation and compared. The results are summarized in Figure 15 for  $(1 - \lambda)_{\Delta H}$  less than 0.6. In this figure  $(1 - \lambda)_d = (1 - \lambda)_{\Delta H}$  is represented by the dashed line. The two solid lines represent the experimental results taken from the previous work, and the curves merge at the higher levels of crystallinity. The upper line represents the previous results for samples with poorly organized structures; the lower line, essentially the  $45^{\circ}$  line, represents a-type spherulites and organized rodlike structures. The points plotted, described by the appropriate symbol, only represent data from the present work. These new data points are all close to, or on, one of the two solid lines. However, contrary to previous conjecture, the appropriate curves appear to be more dependent on the molecular weight than on the morphology. For example, all the samples for fraction  $M_w = 1.61 \times 10^5$  lie very close to the line originally assigned to highly organized supermolecular structures. However, for this fraction these samples include well-developed and poorly developed spherulites as well as ran-

Table V  
Peak Melting Temperatures of Polyethylenes

sample	quenching temp, °C	peak melting temp, °C	crystalline morphology
A. Branched Samples			
a	-70	114.9 ± 0.2	"h"
	20	115.2 ± 0.2	
	35	115.2 ± 0.2	"c"-type spherulites
	45	115.5 ± 0.2	"b"-type spherulites
	60	115.3 ± 0.2	
	72	114.9 ± 0.2	"a"-type spherulites
83	114.8 ± 0.2		
100	114.5 ± 0.2		
g	-70	105.0 ± 0.5	"h"
	65	105.0 ± 0.5	
	80	104.7 ± 0.5	"c"-type spherulites
P108	95	103.8-105.8	
	-70	97.9-99.8	"h"
	0	97.8-98.8	
	38	98.2-100.5	"c"-type spherulites
	50	98.3-99.8	
	68	99.5-100.8	
86	100.3-100.8	"c"-type spherulites	
B. Linear Fractions			
4.6 × 10 <sup>4</sup>	-70	129.9	"b"-type spherulites
	25	128.5	
	44	124.8	"a"-type spherulites
	82	129.8	
1.61 × 10 <sup>5</sup>	100	129.2	"h"
	-129	130.8	
	-70	129.9	"b"-type spherulites
	-30	130.0	
	0	130.2	"a"-type spherulites
	40	129.8	
1.89 × 10 <sup>6</sup>	60	129.7	"h"
	86	130.7	
	100	130.3	"c"-type spherulites
	110	130.3-131.8	
	-70	126.6 ± 0.5	"h"
	0	125.8 ± 0.5	
23	127.0 ± 0.5	"c"-type spherulites	
65	126.3 ± 0.5		
100	126.8 ± 0.5	"b"-type spherulites	

dom lamellae. Samples from a fraction  $M_w = 1.88 \times 10^5$  with disordered structures also are very close to the line. Thus this straight line is not limited to samples with well-organized supermolecular structures. As is indicated in the figure, we find that the results for  $M \geq 5 \times 10^5$ , which only forms poorly organized structures, are close to the upper line. In the range of crystallinities in question, the upper curve appears to be limited to high molecular weights and concomitantly disordered structures. The lower curve contains data for both the ordered and disordered supermolecular structures that can be developed in the lower molecular weight range. The molecular weight influences the relation between  $(1 - \lambda)_d$  and  $(1 - \lambda)_{\Delta H}$  in a manner that cannot be simply envisioned.

With respect to the branched polymers, a comparison of the degree of crystallinity obtained from the density and enthalpy of fusion for both the unfractionated as well as the fractionated samples shows that within experimental error the difference is constant ( $0.10 \pm 0.02$ ), irrespective of morphology, molecular weight, and branching concentration. The branching is thus the dominating factor in governing the properties.

**Melting Temperatures.** The melting temperatures of selected samples, with different morphologies, and in some cases the same levels of crystallinity, have also been studied. These results are tabulated in Table VA for the branched samples and in Table VB for the linear fractions. For present purposes the melting temperatures are re-

corded as the endotherm peaks. Since melting-recrystallization processes should be minimized for the relatively rapid heating rate of 20 K/min, these results are meaningful for comparison within a given sample but not necessarily between samples. The main interest is to examine any relationship between the stability of the crystallite and morphological form actually developed. The main conclusions can be seen by examining the tabulated data for the branched samples. For a given sample, the melting temperatures of the nonisothermally crystallized samples are not sensibly affected, within the experimental error, by the quenching temperature and supermolecular structure. These results are consistent with the previous report.<sup>10</sup> The melting temperatures for the isothermally crystallized samples were found to be several degrees higher, while those for the quenched samples are close to those reported here. As expected, as the branching concentration increases, the melting temperature decreases.

The linear fractions show essentially the same behavior. For example, for  $M = 1.61 \times 10^5$ , a-, b-, and h-type morphologies are observed for different quenching temperatures which yield the same level of crystallinity. The peak melting temperatures are essentially unchanged despite this wide variation in crystalline morphology. The other two linear fractions studied in detail,  $M = 4.62 \times 10^4$  and  $M = 1.89 \times 10^6$ , show the same invariance in melting temperature and crystalline morphology.

### Summary and Conclusions

The crystallization procedure adopted here, namely, nonisothermal rapid crystallization, has not yielded any new type of supermolecular structures beyond those previously reported.<sup>4,5,8</sup> It is, however, now possible to develop a random lamella structure for much lower molecular weight linear polyethylene fractions than has been accomplished heretofore. These structures can also be formed for a variety of low-density (branched) polyethylenes as well as ethylene copolymers. In addition, for properly chosen crystallization conditions, a given molecular weight fraction can display all the known supermolecular structures for polyethylene at a constant level of crystallinity. Previously, one has only been able to achieve these different structures at a constant crystallinity by varying the molecular weight.<sup>8</sup> Thus the level of crystallinity, the molecular weight, and the supermolecular structures can now be treated as independent variables in analyzing the factors which influence the properties of semicrystalline polymers.

The detailed studies of thermodynamic properties such as density, enthalpy of fusion, and observed melting temperatures make clear that they are independent of the supermolecular structure. These results are consistent with previous ones limited to isothermally crystallized samples.<sup>8</sup> The crystallization temperature, or crystallization conditions, appears to be the major determinant of these properties. This is most probably due to the influence of the lamellae, or crystallite thickness, and its relation to nucleation control. On the other hand, it still remains to be investigated whether mechanical and deformation properties are sensitive to the supermolecular structure while the other independent variables are held constant.

Having established the conditions, in terms of crystallization temperature and molecular constitution, for the development of the different supermolecular structures, it is important to seek the mechanistic basis for the formation of the different morphological forms. We outline here some of the underlying structural features for molecular weight fractions and some of the principles that must be applicable. In essence, this process involves ex-

plaining the crystalline morphology in terms of the crystallization kinetics and mechanisms. When a very molecular weight limited, isothermal-crystallization range is examined, there is a well-defined set of temperatures where the temperature coefficient of the overall crystallization rate<sup>29</sup> and the growth rate of spherulites or rodlike structures<sup>6</sup> change by a factor of 2 for linear polyethylene. Crystallization above and below this set of temperatures has been termed regime I and regime II, respectively.<sup>6</sup> This phenomenon is, however, restricted to the molecular weight range  $1 \times 10^6 \gtrsim M \gtrsim (2-4) \times 10^4$ . Morphologically, the high-temperature region (regime I) corresponds to rodlike forms (g morphology), while regime II corresponds to b- and c-type spherulites.<sup>6</sup> Thus there appears to be a causal relation between the morphological form observed at a given temperature and the temperature coefficient of the crystallization. The theoretical explanation for the temperature coefficient difference<sup>6,37</sup> is virtually identical with the much earlier work of Hillig<sup>38</sup> for low molecular weight substances. In this calculation, the factor of 2 results when one assumes that in regime I the rate of lateral growth of a nucleus is very much faster than the nucleation rate per unit area. In regime II, in contrast, new growth steps nucleate before the layer is completely filled,<sup>6,37,38</sup> i.e., multiple nucleation occurs on a growing face. To correlate this formal kinetic analysis with the concomitant morphological results, it can be postulated that this multiple nucleation leads to spherulite formation through some type of noncrystallographic growth. On the other hand, when a layer is filled by a single nucleation step, as would be favored by high crystallization temperatures and low molecular weights, crystallographically controlled growth can be approached, leading to rod- or sheetlike habits.<sup>15</sup> These arguments are based on the implicit premise of interface-controlled growth.<sup>42</sup>

For higher molecular weight  $M \gtrsim 2 \times 10^6$ , the overall crystallization kinetics are consistent with a diffusion-controlled growth mechanism.<sup>29</sup> Over this molecular weight range, randomly oriented lamellae are observed under all crystallization conditions so that no organized supermolecular structures are found. The temperature coefficient for the overall crystallization rate of the high molecular weight fractions is the same as for the low molecular weight samples at high temperatures. In the latter case, rodlike aggregates of lamellae are formed. These results imply that the temperature coefficient of lamella growth is the same in both cases. There is also a strong inference in the high molecular weight results that diffusion-controlled growth inhibits the formation of spherulitic structures. This concept is further supported by the fact that when the high molecular weight nonspherulitic samples are swollen in diluent at elevated temperatures, spherulites are observed subsequent to drying and cooling.<sup>7</sup>

This principle of diffusion-controlled growth influencing crystalline morphology can be carried over to the very rapidly crystallized samples. Under these conditions, poorly developed spherulites and random structures are observed at much lower molecular weights as compared to crystallization occurring isothermally at elevated temperatures. Because of the temperature, the initiation of new lamellae will be greatly enhanced at the very large, although undefined, undercooling. The large number of centers reduces the number of sequences available for deposition on the face of any given growing lamella, and the low temperatures will reduce the growth rates. The net effect is that of essentially diffusion-controlled growth.

Thus there are several different fundamental growth processes and their interplay, which determine the crys-

talline morphology. There also seems to be a general principle emerging that diffusion-controlled growth retards the development of any organized supermolecular structures. Diffusion control can be introduced by different constitutional and crystallization factors, such as high molecular weights, high co-unit or branching concentrations, or crystallization at large undercooling, i.e., very rapidly. Thus the disorganized structures of randomly organized lamellae can result from different causes and lead to differences in the details of fine structure. An example is seen in the electron micrographs of Figure 5, where random structures of the same sample are shown but where there are differences in the lamella fine structures.

In contrast, it would appear that when interface control is operative, then either spherulites of various levels of perfection or rodlike or sheetlike structures are formed. Organized structures are again formed, the details of which depend also on constitutional and kinetic factors. These symmetric studies have set forth the general principles involved and have sorted out the different governing factors. It remains now to quantify these conclusions in a unified manner.

**Acknowledgment.** Support of this work by the Exxon Chemical Corp. is gratefully acknowledged. We also thank R. Allen and G. Stack for experimental assistance.

## References and Notes

- (1) Mandelkern, L. *J. Phys. Chem.* **1971**, *75*, 3909.
- (2) Mandelkern, L. "Characterization of Materials in Research: Ceramics and Polymers"; Syracuse University Press: Syracuse, N.Y., 1975; Chapter 13.
- (3) Mandelkern, L. *Acc. Chem. Res.* **1976**, *9*, 81.
- (4) Mandelkern, L. *Discuss. Faraday Soc.* **1980**, No. 68, 310.
- (5) Go, S.; Prud'homme, R.; Stein, R. S.; Mandelkern, L. *J. Polym. Sci., Polym. Phys. Ed.* **1974**, *12*, 1185.
- (6) Hoffman, J. D.; Frolen, L. J.; Ross, G. S.; Lauritzen, J. I., Jr. *J. Res. Natl. Bur. Stand., Sect. A* **1975**, *79*, 671.
- (7) Mandelkern, L.; Go, S.; Peiffer, D.; Stein, R. S. *J. Polym. Sci., Polym. Phys. Ed.* **1977**, *15*, 1189.
- (8) Maxfield, J.; Mandelkern, L. *Macromolecules* **1977**, *10*, 1141.
- (9) Mandelkern, L. *Discuss. Faraday Soc.* **1980**, No. 68, 365.
- (10) Mandelkern, L.; Maxfield, J. *J. Polym. Sci., Polym. Phys. Ed.* **1979**, *17*, 1913.
- (11) Mandelkern, L.; Glotin, M., to be submitted for publication.
- (12) Jackson, J. B.; Flory, P. J. *Polymer* **1964**, *5*, 159.
- (13) Stein, R. S. "New Methods of Polymer Characterization"; Ke, B., Ed.; Wiley-Interscience: New York, 1964.
- (14) Stein, R. S. "Structure and Properties of Polymer Fibers"; Lenz, R. W.; Stein, R. S., Eds.; Plenum Press: New York, 1972.
- (15) Voigt-Martin, I. G.; Mandelkern, L.; Fischer, E. W. *J. Polym. Sci., Polym. Phys. Ed.*, in press.
- (16) Fatou, J. G.; Mandelkern, L. *J. Phys. Chem.* **1965**, *69*, 71.
- (17) Chiang, R. *J. Polym. Sci.* **1959**, *36*, 91.
- (18) Axelson, D. E.; Levy, G. C.; Mandelkern, L. *Macromolecules* **1979**, *12*, 41.
- (19) Bovey, F. A.; Schilling, F. C.; McCracken, F. L.; Wagner, H. L. *Macromolecules* **1976**, *9*, 76.
- (20) We thank Dr. L. Westerman for furnishing these results and samples.
- (21) Westerman, L.; Clark, J. C. *J. Polym. Sci., Polym. Phys. Ed.* **1973**, *11*, 559.
- (22) Hser, J.-C.; Carr, S. H. *Polym. Eng. Sci.* **1979**, *19*, 436.
- (23) Benson, R. A. Ph.D. Dissertation, Florida State University, Aug 1978.
- (24) Prud'homme, R. F.; Yoon, D. Y.; Stein, R. S. *J. Polym. Sci., Polym. Phys. Ed.* **1973**, *11*, 1047.
- (25) Moutani, M.; Hayashi, N.; Utsuo, A.; Kawai, H. *Polym. J.* **1971**, *2*, 74.
- (26) Chiang, R.; Flory, P. J. *J. Am. Chem. Soc.* **1961**, *83*, 2057.
- (27) Mandelkern, L.; Allou, A. L., Jr.; Gopalan, M. *J. Phys. Chem.* **1968**, *72*, 309.
- (28) Mandelkern, L.; Fatou, J. G.; Denison, R.; Justin, J. *J. Polym. Sci.* **1965**, *3*, 803.
- (29) Ergoz, E.; Fatou, J. G.; Mandelkern, L. *Macromolecules* **1972**, *5*, 147.
- (30) Flory, P. J. *J. Chem. Phys.* **1949**, *17*, 223.

- (31) Flory, P. J. *Trans. Faraday Soc.* **1955**, *51*, 845.
- (32) Otocka, E. P.; Roe, R. J.; Bair, H. E. *J. Polym. Sci., Polym. Phys. Ed.* **1974**, *12*, 1245.
- (33) Mandelkern, L. "Crystallization of Polymers"; McGraw-Hill: New York, 1964.
- (34) Strobl, G. R.; Hagedorn, W. *J. Polym. Sci., Polym. Phys. Ed.* **1978**, *16*, 1181.
- (35) Jackson, J. F.; Mandelkern, L. "Analytical Calorimetry"; Johnson, J. F., Porter, R. S., Eds.; Plenum Press: New York, 1968; Vol. 1, p 1.
- (36) Sakaguchi, F.; Maxfield, J.; Mandelkern, L. *J. Polym. Sci., Polym. Phys. Ed.* **1976**, *14*, 2137.
- (37) Lauritzen, J. I., Jr. *J. Appl. Phys.* **1973**, *44*, 4353.
- (38) Hillig, W. B. *Acta Metall.* **1966**, *14*, 1868.
- (39) We thank Dr. I. Voigt-Martin for kindly supplying us with the electron micrographs.
- (40) The previously reported SALS patterns for this series of quenched samples<sup>10</sup> indicates that the quenching temperature corresponded to about 70 °C.
- (41) Our previous report<sup>10</sup> suffers from this deficiency, and the enthalpies of fusion are lower than the correct values. This error can be rectified, to a very good approximation, by adding 0.10 to the degree of crystallinities previously calculated from the enthalpy of fusion measurements.
- (42) It should be noted that the premise of interface-controlled growth makes no assumption or imposes any requirements on the interfacial structure. In particular, identification with a regularly folded interface is unnecessary and incorrect.

## Hydrophobic Domain Structure of Water-Soluble Block Copolymer. 1. Analysis of the Structure of the Polymolecular Micelle

**Masahisa Ikemi,<sup>1a</sup> Nobuyuki Odagiri,<sup>1a</sup> Shinobu Tanaka,<sup>1a</sup> Isao Shinohara,<sup>\*1a</sup> and Akio Chiba<sup>1b</sup>**

*Department of Polymer Chemistry and Department of Applied Physics, Waseda University, Ohkubo, Shinjuku-ku, Tokyo 160, Japan. Received July 28, 1980*

**ABSTRACT:** Small-angle X-ray scattering and fluorometric measurements were carried out on an aqueous solution of the water-soluble ABA-type block copolymer of poly(2-hydroxyethyl methacrylate) (PHEMA) and poly(ethylene oxide) (PEO) to study micelle formation of the water-soluble block copolymer and its hydrophobic domain structure. The water-soluble block copolymer formed polymolecular micelles above ca. 0.1 g/dL and the hydrophobicity of the block copolymer was enhanced accompanied by intermolecular association. A spherical micelle model with a boundary region was proposed and a theoretical particle scattering function was derived for this model to compare with the experimental curve. The polymolecular micelle appeared to be constructed from a large number of molecules and the PHEMA core of the micelle was significantly large. The enhanced hydrophobicity is believed to result from aggregation of the PHEMA blocks within the interior core. The X-ray scattering data reveal that a large boundary region of the constituent blocks exists in the interfacial region between the core and the shell and that the ratio of half the boundary width to the core radius reached ca. 0.3. It is suggested that the hydrophobicity of the aggregated core is remarkably affected by intermixing of the constituent blocks.

### Introduction

A water-soluble block copolymer composed of both hydrophobic and hydrophilic blocks is expected to possess characteristic properties,<sup>2,3</sup> and study of the structure and properties of such a block copolymer in water has attracted extensive attention. In particular, application to biomedical materials is of interest because the water-soluble block copolymer can completely restrict the aggregation and anticomplementary activity of human immunoglobulin.<sup>3</sup> The solution behavior of block copolymers in organic solvents has been studied,<sup>4-9</sup> but only a few papers have been published on water-soluble block copolymers.

Water-soluble amphiphilic polymers form hydrophobic regions effectively in water, due to the hydrophobic interaction between the nonpolar groups.<sup>10-12</sup> It has been suggested that the hydrophobic regions of polymers are affected, among other things, by factors such as the chemical structure of both the hydrophobic and the hydrophilic groups and their ratio in the copolymers.<sup>13,14</sup>

In a previous paper<sup>2</sup> we described the preparation of a water-soluble ABA-type block copolymer of hydrophobic poly(2-hydroxyethyl methacrylate) (PHEMA) and hydrophilic poly(ethylene oxide) (PEO) and discussed the hydrophobic region of the monomolecular block copolymer in dilute aqueous solution based on the results of fluorometric measurements with 8-anilidonaphthalene-1-sulfonate (ANS) as a fluorescent probe for hydrophobicity.

The mode of arrangement of the constituent segments along the chain considerably affects the hydrophobic regions, and the block copolymer formed regions of strong hydrophobicity as compared with the corresponding random copolymer.

On the other hand, there is clear evidence of polymolecular micelle formation due to intermolecular association in the water-soluble ABA-type block copolymer described above. For the structure of intermolecular associates of block copolymers in organic solvents, a spherical micelle model has been proposed;<sup>15-19</sup> i.e., the aggregated insoluble chains are surrounded by the expanded soluble chains. Most of them are of the completely segregated type comprising two concentric spheres. It has been pointed out,<sup>19</sup> however, that considerable intermixing of the constituent blocks must take place for the solvent-swollen micelles in dilute solution.

We investigate in this article the structure and the hydrophobic regions of the intermolecular associates of the water-soluble block copolymer composed of hydrophobic PHEMA and hydrophilic PEO by means of small-angle X-ray scattering and fluorometric measurement using a fluorescent probe. A structural model for the intermolecular associate having an interfacial region between the core (PHEMA blocks) and the shell (PEO blocks) is proposed. The theoretical scattering functions are derived for this model and compared with the experimental results. The relation between the hydrophobic region and the